FE Simulation Applied to the Vibration of Hydraulic Pipes

Eduardo Machado da Conceição Rodrigues Pereira
eduardo.rodrigues.per@gmail.com

Instituto Superior Técnico, Universidade de Lisboa, Portugal

December 2021

Abstract

The structural vibration in a hydraulic or gas pipeline system can be strongly affected due to multi-source excitation of high fluid pressure fluctuation inside the pipes. Understanding the vibration behavior is the first step to controlling the vibrations in the pipeline with common vibration control technologies to ensure the safety of the pipe system and machinery. The common vibration control technologies have been demonstrated to be effective in typical structures as aerospace structures and gas pipeline structures. Both acoustic induced vibration and flow induced vibration can be a cause of failure and both types of vibration use different methods to perform the vibration analysis. The structural vibration analysis of three-dimensional pipelines conveying fluid is modeled by the finite element method (FEM) based on Euler-Bernoulli and Timoshenko beam theories and the transfer matrix method (TMM) used for the one-dimensional acoustic pressure waves solution and to represent the acoustic-structure interaction in a pipeline as a weak or one-way coupled system. This fluid-structure interaction in compliant piping systems is modeled by extended water hammer theory for the fluid and beam theory for the pipe structure. A source code was developed in MATLAB to predict the dynamic behavior of three-dimensional complex and simple pipe systems subjected to harmonic and acoustic external loads or resonant frequencies of complex pipe networks conveying steady fluid flow. From the displacement and pressure fields optimal layout technique of pipeline using clamps can be archived to reduce vibration amplitudes.
Keywords: Finite element method, Transfer matrix method, Fluid-structure interaction, Acoustics, Euler-Bernoulli beam theory, Timoshenko beam theory

1. Introduction

Pipelines are essential structural systems to transport all types of liquid fluids and gases, and can range from the very simple ones to a more complex ones. They can be simple as a single pipe conveying fluid from one reservoir to another and more elaborate as a complex transport of natural oil or gas in a major metropolitan area, containing several kinds of pumps, valves, branches and supporting parts. Pipelines can also be made with small diameters pipes like in the hydraulic pipelines in airplanes and cars, and larger diameters for long distance gas transport, for example. One of the major causes of failures or downtime is associated with vibration of these structures and controlling these vibrations is the challenging work to ensure a normal operation of the pipeline or the flight safety of an aircraft. Excessive vibration, that usually involves the lateral vibration of the pipeline and the shell wall radial vibrations. At low frequencies, pipe vibration occurs laterally, like a beam, and at higher frequencies, the pipe shell wall starts to vibrate radially across its cross-section.

Piping configuration, number and type of supports, span length, or material affect vibration levels and can be modified to make the system acceptable. To understand what can be changed its important to know all the principle mechanisms and excitation sources that vibrates the structure.

The pipelines are subjected to various types of vibration in their lifetime. Pipelines can transport gas for supplying energy by combustion process and for other processes that involve high pressure gas transportation through the pipes and other related components. Another practical use of pipelines is in aircraft hydraulic systems. This is a typical high-pressure and high-speed system that includes supporting parts, such as brackets or clamps, where, due to multi-source excitation of high fluid pressure fluctuations can cause unwanted vibrations [1]. In aeronautical applications, space constraint is rigorous and given the large number of pipelines collision between adjacent pipes also leads to the potential damage. These movement vibrations may result in fatigue damage to the pipeline structure and damage to pipeline supports. These vibrations can

be lateral pipeline vibration due to low frequency or high frequency piping shell wall vibrations that can be caused by excitation of circumferential radial frequency modes. Failure modes of hydraulic pipeline system includes excessive vibration and fatigue. This occurs due to pipeline resonance. That is, when the fluid pulsation frequency or external excitation are similar to the pipeline natural frequencies. During this resonance, damage may occur due to high vibration stress, and then a crack may open and propagate.

OpenPulse is used to verify the developed MATLAB code in the acoustic section. *OpenPulse* [2] is a open source software for pulsation analysis of pipeline systems written in Python for numerical modelling of low-frequency acoustically induced vibration in gas pipeline systems.

2. Background

2.1. Euler-Bernoulli and Timosheko beam theory
To model a pipeline, a three-dimensional beam element is used, and each element contain two nodes and every node has six degrees of freedom: three translational displacements and three rotational degrees of freedom (Figure 1).

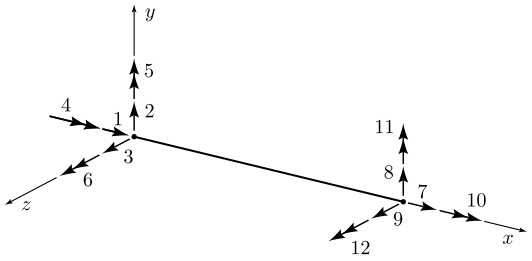

Figure 1: Element with 12 degrees of freedom

The displacements of a point in a cross section are described by the translation components, w_x, w_y, w_z, of the neutral line and the rotations, θ_x, θ_y, θ_z of the cross section. It is considered that w_i are small compared by beam length and the rotation components are all small so that $\sin\theta \approx \tan\theta \approx \theta$.

Euler-Bernoulli beam kinematics [3, 4] assumes that a cross-section remains orthogonal to the deformed beam axis. If the rotation is equal to the slope of the beam, then

$$\theta_y = -\frac{dw_z}{dx}, \quad \theta_z = \frac{dw_y}{dx} \tag{1}$$

Timoshenko beam theory differs from Euler-Bernoulli theory because it accounts for shear deformation. The rotation of plane section orthogonal to beam axis is given by

$$\theta_y = -\frac{dw_z}{dx} + \gamma_{xz}, \quad \theta_z = \frac{dw_y}{dx} - \gamma_{xy} \tag{2}$$

where dw/dx is the slope of the beam axis and γ is the rotation due to the distortion of the cross-section.

With the shape functions defined, for each of the model, the stiffness and mass matrices can be determined. The determination of the damping matrix follows the Rayleigh damping matrix, where this matrix is proportional to the system's mass and stiffness matrices, given by

$$\mathbf{C} = \alpha\mathbf{M} + \beta\mathbf{K} \tag{3}$$

where α is the mass-proportional coefficient and β is the stiffness-proportional coefficient. Now, the damped dynamic equation of motion can be ritten was

$$\mathbf{M}\ddot{\mathbf{u}}(t) + \mathbf{C}\dot{\mathbf{u}}(t) + \mathbf{K}\mathbf{u}(t) = \mathbf{f}(t) \tag{4}$$

With this dynamic equation it is now possible to perform modal and harmonic analysis. The modal analysis is used to calculate natural frequencies and modes of vibration given both stiffness and mass matrices,

$$[\mathbf{K} - \omega^2\mathbf{M}]\mathbf{U} = \mathbf{0} \tag{5}$$

and the harmonic analysis is used to predict the steady state dynamic response of a structure subjected to an harmonic loading,

$$[-\omega^2\mathbf{M} + i\omega\mathbf{C} + \mathbf{K}]\mathbf{U} = \mathbf{F} \tag{6}$$

2.2. Internal Fluid Flow
Considering a pipe with fluid flowing through it at pressure p and at a constant velocity v through the internal cross-section of area A_i. Due to the lateral vibration of the pipeline, the deflected pipe, the fluid is accelerated because of the changing curvature. Forces and moments acting on the fluid and pipe element are shown in figure 2.

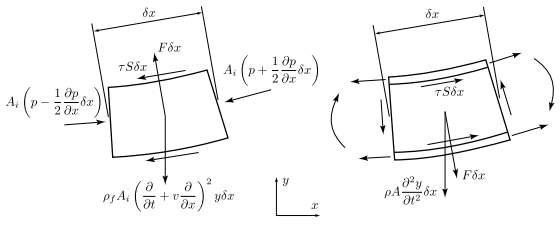

Figure 2: Fluid and pipe forces

Given the forces and moments the derivation of the equation of motion for a free vibration of a fluid

convening pipe is given by equation (2.2). Derivation of this equation is presented in [5] and it is done by a balance of forces in both fluid and pipe element considering small deflections and if gravity, internal damping, externally imposed tension and pressurization effects are either absent or neglected.

$$EI\frac{\partial^4 y}{\partial x^4} + 2\rho_f A_i v\frac{\partial^2 y}{\partial x \partial t} + \rho_f A_i v^2\frac{\partial^2 y}{\partial x^2} + (\rho A + \rho_f A_i)\frac{\partial^2 y}{\partial t^2} = 0 \quad (7)$$

where v is the flow velocity of the fluid and $(\rho A + \rho_f A_i)$ is the total mass per unit length of the pipe. In equation (2.2) the first term is the force component acting on the pipe as a result of bending of the pipe. The second term is the force component acting on the pipe as a result of flow around deflected pipe curvature. The third therm is the force required to rotate the fluid element, also known as Coriolis force. The last term represents the force component acting on the pipe as a result of the inertia of the pipe and the fluid flowing through it. With this equation the stiffness, mass and damping fluid matrices can be constructed and used in both modal and harmonic analysis. The overall stiffness matrix is calculated subtracting the fluid matrix to the structural matrix. This results in a loss of stiffness as the velocity inside the pipeline increases. Global mass and damping matrices are calculated by the sum of fluid matrices to the structural matrices.

2.3. Acoustics

Assuming that the flow is frictionless, no external forces are applied and limit the analysis to acoustic perturbations (ρ', p', $\mathbf{v}'$) at a stagnant uniform fluid (ρ_0, p_0) as

$$p(\mathbf{x}, t) = p_0 + p'(\mathbf{x}, t) \quad (8)$$

$$\rho_f(\mathbf{x}, t) = \rho_{f0} + \rho'_f(\mathbf{x}, t) \quad (9)$$

$$\mathbf{v}(\mathbf{x}, t) = \mathbf{v}'(\mathbf{x}, t) \quad (10)$$

and using the non-dissipative wave equation, the pressure and volume velocity can be calculated inside a tube element.

Considering a straight uniform pipe element with constant fluid properties inside the tube. Pressure and volume velocity or flow rate in the inlet and outlet are denoted as p_1, q_1 and p_2, q_2. The acoustic impedance if the element is represented by Z_f. The first objective is to find a matrix equation that expresses the volume velocity and pressure at any point inside the tube element at the wave number, $k = \omega/c_f$, in terms of their values at the inlet. The tube element can be represented as a linear system with to inputs and two outputs as

$$\begin{bmatrix} p_2 \\ q_2 \end{bmatrix} = \mathbf{T}\begin{bmatrix} p_1 \\ q_1 \end{bmatrix} \quad (11)$$

where $\mathbf{T}$ is the transfer matrix for the uniform tube element and it is given by

$$\mathbf{T} = \begin{bmatrix} \cos(kx) & -i\,Z_f \sin(kx) \\ -i/Z_f \sin(kx) & \cos(kx) \end{bmatrix} \quad (12)$$

where $Z_f = \rho_f\, c_f/A_i$ is the acoustic impedance.

The stiffness matrix relates, in contrast with the transfer matrix, the same type of variables in each nodal vector which is more suitable with the finite element method. This stiffness matrix, $\mathbf{S}$ relates the nodal volume velocities and the nodal pressures as

$$\begin{bmatrix} q_1 \\ q_2 \end{bmatrix} = \mathbf{S}\begin{bmatrix} p_1 \\ p_2 \end{bmatrix} \quad (13)$$

with

$$\mathbf{S} = \begin{bmatrix} -i\cot(kx)/Z_f & i/Z_f \sin(kx) \\ i/Z_f \sin(kx) & -i\cot(kx)/Z_f \end{bmatrix} \quad (14)$$

2.4. Fluid-Structure Interaction

Fluid-structure interaction is a dynamic phenomenon that causes a compliant system to move when pressure waves exert forces on the structure. This interaction is always caused by dynamic forces which act on fluid and pipe and can be divided into two main groups [6, 7]: distributed forces and local forces. Forces that act along the pipe are called distributed forces and it is caused by the fluid pressure what causes the pipe to develop axial stresses in the walls. This is refereed as Poisson coupling in connection with the Poisson coefficient, ν, that transform radial and hoop stresses into axial stress by the generalized Hook's law. Forces caused by fluid friction in the pipe walls are also distributed forces and are called friction coupling. Local forces act at specific points in a pipe system such as unrestrained valves, bends and tees and is generally more dominant compared with the other coupling mechanisms.

First, considering only internal pressure in the pipe system the radial and circumferential stresses can be expresses as

$$\sigma_{rr} + \sigma_{\theta\theta} = \frac{2p(\omega)D_i^2}{D_e^2 - D_i^2} \quad (15)$$

Given the stress-strain relations, the axial strain, ϵ_{xx}, generated by the internal pressure on a open tube element is

$$\epsilon_{xx} = \frac{1}{E}[\sigma_{zz} - \nu(\sigma_{rr} + \sigma_{\theta\theta})] \quad (16)$$

with $\sigma_{zz} = 0$ for an open ended pipe element.

The most important interaction mechanism is junction coupling. In most of the times, a pipe network consists of straight sections of pipe connected by elbows, tees and diameter changes. The local forces on this sections of pipe can be calculated with help from the Reynolds transport theory applied for momentum conservation. For the equilibrium to be archived pipe internal forces need to compensate the vector sum of the pressure forces. Figure 3 illustrates an elbow with pressure and change in momentum forces that are compensated by internal pipe stresses.

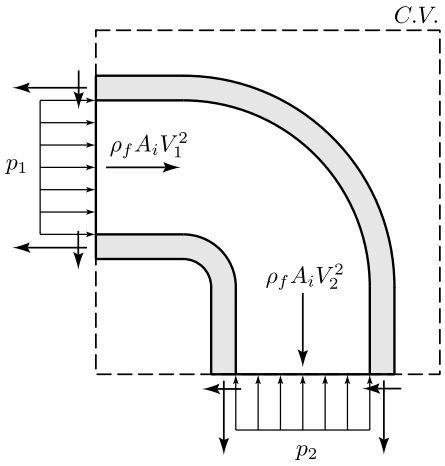

Figure 3: Elbow control volume

3. Implementation

3.1. Mesh

The program developed uses a text document, created by the user, to import the mesh. This document contains all the relevant information about node locations, element connectivity, element refinement, corner locations and corner radius. However, it is only necessary to provide an initial scheme of the final mesh (Figure 4), containing only straight lines.

Mesh refinement is introduced to define more points along a single straight segment or to define a corner with line segments. This refinement is done element by element and corner by corner given the number of intermediate points each of the initial elements has. The final mesh (Figure 5) is obtained by the program after performing all the operations of node numbering, node connectivity between the nodes and then calculating their coordinates. Next it will be explained all this process, starting from establishing element, given the initial user input element connectivity and refinement parameters, and then calculating node coordinates.

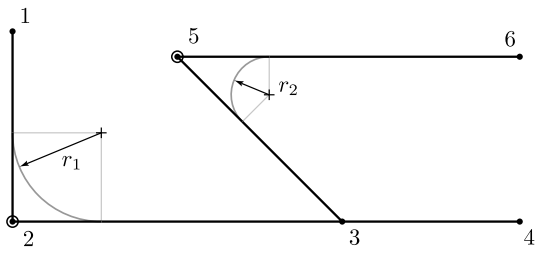

Figure 4: Initial mesh design with user input control points

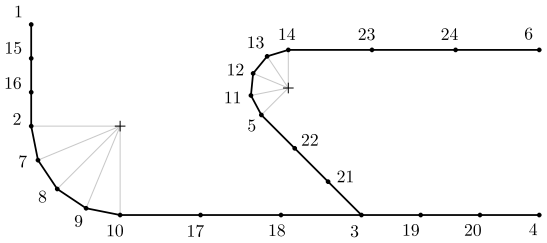

Figure 5: Final mesh with refinement and node numbering

Calculating node coordinates for straight line elements is straight forward . Given the line start and end points, A and B respectively, and the number of segments the element is going to be divided into, N_s, the new points coordinates are easily calculating dividing the segment between the two nodes.

A more difficult and time-consuming process is to determine nodal coordinates for the nodes that form corners. Given the corner node, C, both adjacent nodes, A and B, and corner radius, r, it is possible to calculate the arc start, S, end, E, and centre point, O (Figure 6).

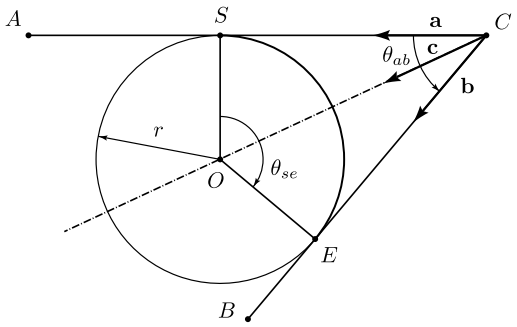

Figure 6: Important points and corner geometry

The new points are calculated rotating the vector that connects O to S multiple times until the desired refinement is obtained.

3.2. Transformation matrix

To transform the element matrices into the global coordinate system it is required a transformation of each element to account for the differences in orientation of all local coordinate systems in three-dimensional space. Different authors use different methods to develop element transformation matrix in spatial coordinates. It was implemented a method based on [8, 9].

The transformation matrix $\mathbf{T}$ to transform local vector into global vector is given by

$$\mathbf{T} = \begin{bmatrix} \mathbf{R}_{(3\times3)} & \mathbf{0} & \mathbf{0} & \mathbf{0} \\ \mathbf{0} & \mathbf{R}_{(3\times3)} & \mathbf{0} & \mathbf{0} \\ \mathbf{0} & \mathbf{0} & \mathbf{R}_{(3\times3)} & \mathbf{0} \\ \mathbf{0} & \mathbf{0} & \mathbf{0} & \mathbf{R}_{(3\times3)} \end{bmatrix} \tag{17}$$

where $\mathbf{T}$ is a 12×12 symmetric matrix given the twelve degrees of freedom per element. The submatrix $\mathbf{R}$ is given as

$$\mathbf{R} = \begin{bmatrix} l & m & n \\ -\dfrac{m}{D} & \dfrac{l}{D} & 0 \\ -\dfrac{ln}{D} & \dfrac{mn}{D} & D \end{bmatrix} \tag{18}$$

with

$$\frac{x_2 - x_1}{L} = l \tag{19}$$

$$\frac{y_2 - y_1}{L} = m \tag{20}$$

$$\frac{z_2 - z_1}{L} = n \tag{21}$$

and $D = (l^2 + m^2)^{1/2}$.

3.3. Fluid-Structure Interaction

Identification of the forces involved in the fluid-structure interaction was performed. From that, the only forces at it will be taken into account are the Poisson coupling force and the junction coupling force. Since, from the acoustic harmonic analysis the nodal pressures are calculated some approximations have to be perform to calculate the forces originated from those pressures. Poisson coupling force assumes a constant pressure along a pipe element, the average pressure at an element needs to be calculated to calculate the nodal forces that arise from the coupling mechanism. This average pressure is also used to calculate the forces acting on the nodes. The force acting on the nodes for given element is,

$$\mathbf{F} = [-F_x, 0, 0, 0, 0, 0, F_x, 0, 0, 0, 0, 0]' \tag{22}$$

where F_x is given sum of local pressure forces and the distributed Poisson coupling force, that is

$$F_x = p_{avg} A_i + A(-\nu(\sigma_{rr} + \sigma_{\theta\theta})) \tag{23}$$

This approach is possible because it accurately represents the forces acting on pipelines when changes in velocity (speed or direction) occurs. For example, figure 7 from [10] shows different common pipeline sections and the forces acting on them given fluid the pressures.

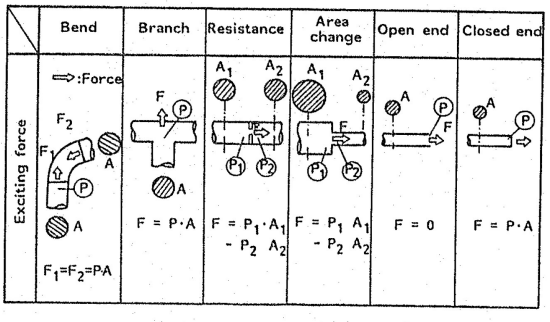

Figure 7: Piping sections excited by pressure pulsation [10]

4. Results

4.1. Structural Results

The differences between Euler-Bernoulli and Timoshenko beam models are now analysed. The comparison between these models and analytical result is also presented. For the three first modes of vibrations of a pinned-pinned pipe, the natural frequencies for each mode is calculated for an increasing number of elements in the FEM model. For the first mode, figure 8, the theoretical value based in Euler-Bernoulli model is represented with a grey margin representing a plus and minus percentage of that value.

The Timoshenko model gives smaller natural frequency than the Euler-Bernoulli as predicted given the reduced stiffness of the model. With 6 elements the Euler-Bernoulli model is inside that analytical margin. For the second and third modes, respectively given in figures 9 and 10, the differences between FEM models is more significant, seen by the grey margins. Also, it takes more elements to archive the same error margins, 12 elements for the second mode and 16 for the third.

Now, the default length of the pipe is reduced without modifying the cross-section geometry to study the influence of the pipe thickness-to-length ratio in both Euler-Bernoulli and Timoshenko beam theories. Instead of thickness it has used the gyration radius to better describe the section geometry.

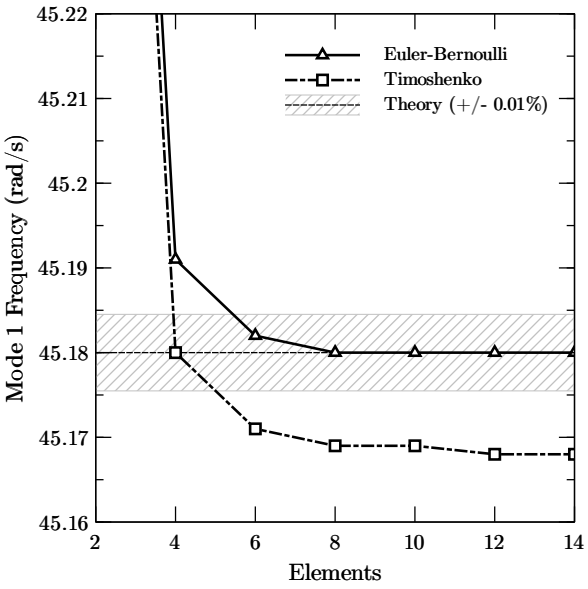

Figure 8: Mode 1 natural frequencies for pinned-pinned pipe

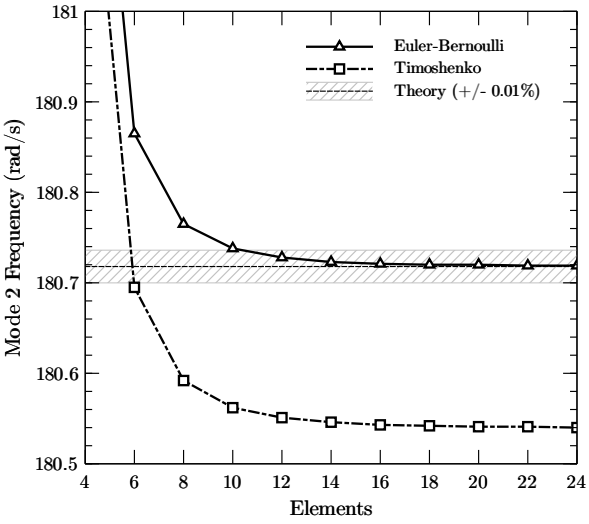

Figure 9: Mode 1 natural frequencies for pinned-pinned pipe

Figure 11 shows the ratio of frequencies between FEM models for the first three vibration frequencies for an decreasing pipe length.

These results show that the Timoshenko theory results are very similar to the Euler-Bernoulli results when r_x/L is small, however, the results show that the difference between theories tends to grow larger for a thicker beam.

Another method to compare the two models developed with *OpenPulse* an harmonic analysis was performed. For this, a unit force was applied to the free end of L shape pipe with clamped-free boundary conditions. This force acts parallel to the pipe

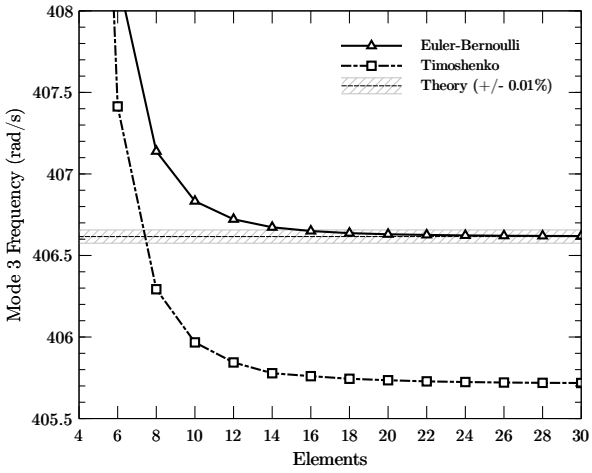

Figure 10: Mode 1 natural frequencies for pinned-pinned pipe

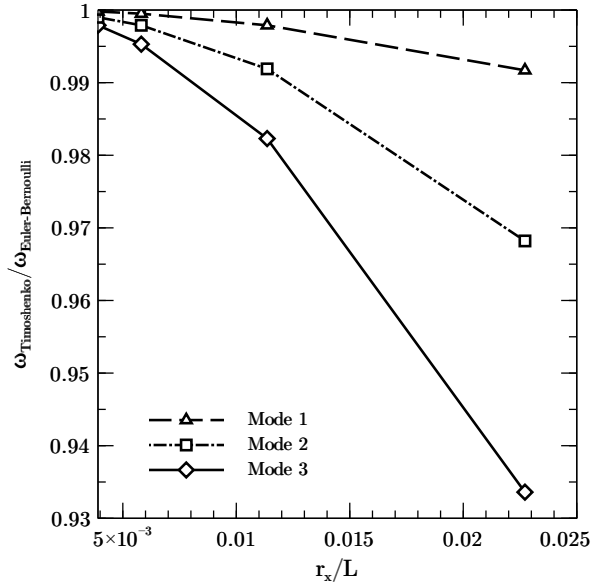

Figure 11: Length influence in FEM structural models with 20 elements

plane and acts orthogonal to free end pipe. Figure 12 shows structural response for a frequency from 0 to 100 Hz. From this graph is possible to identify the resonant frequencies, corresponding to in-plane natural frequencies of modes 2 and 4. A anti-resonant frequency is located at around 62 Hz. It is possible to see the larger stiffness from the Euler-Bernoulli theory and how close the developed Timoshenko model is to the *OpenPulse* model.

4.2. Steady Internal Flow Results

Now, the results of the vibration of a pipe with fluid flow are presented. First, it is shown the results comparing it to the experiment performed by [11]. In that experiment, the objective was to study

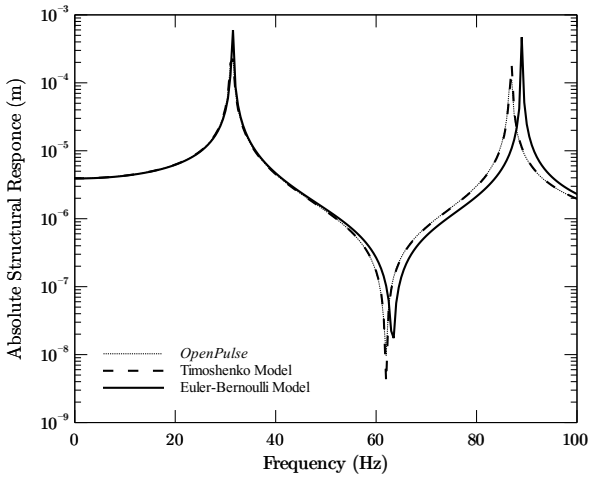

Figure 12: Structural response (in-plane) of free end with a transverse unit applied force

the effect of high-velocity fluid flow on the bending vibrations and stability of a simple supported pipe. To investigate free vibrations, the pipe transporting different fluid velocities, a small disturbance to the pipe was necessary. In figure 13, where it can be seen that the model follows the experimental results with some precision. As predicted, the system becomes unstable which results in permanent deformation of the pipe [11]. The velocity for which the system becomes unstable, or $\omega = 0$, is called critical flow velocity.

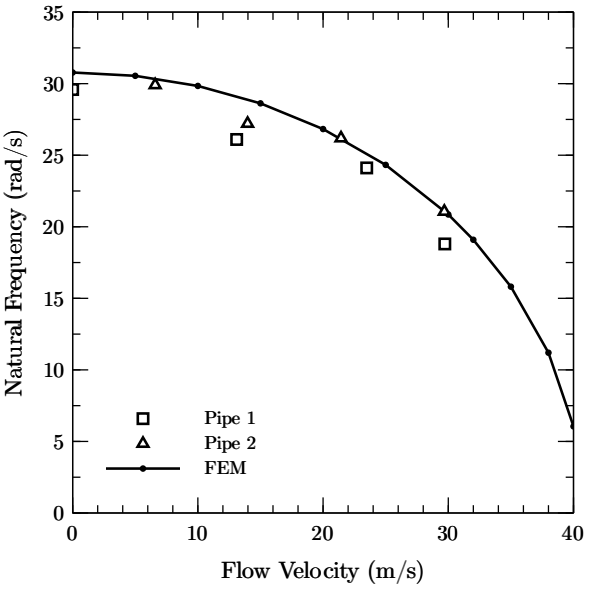

Figure 13: Lowest natural frequency of the simply supported straight pipe

Now, this fluid flow model is compared with a model proposed by [12]. This proposed method considers a slender fluid-structure system, consisting of an elastic pipe with a compressible, viscous fluid. A finite element computer program was developed that makes possible to represent a pipe as a frequency dependent elasto-acoustic element. For this comparison, a cantilever pipe conveying fluid is used. This system is excited by a unit transverse force at the free. The response of the pipe free end in the direction of the force is presented in figure 14 for flow velocities of $V = 0\,m/s$ and $V = 50\,m/s$.

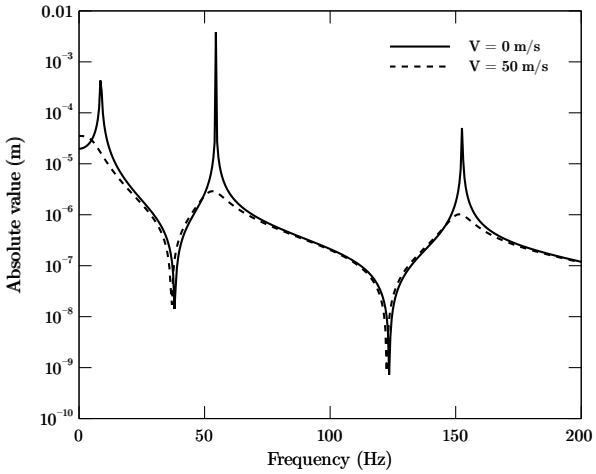

Figure 14: Transverse displacement of the free end

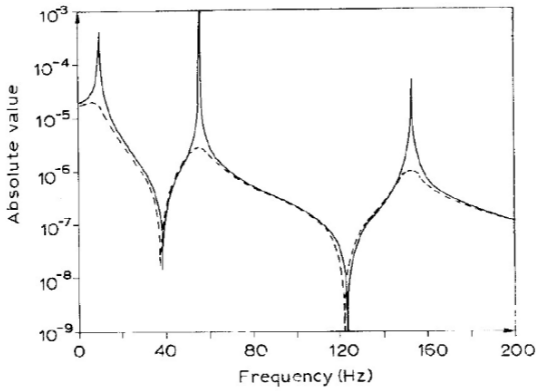

Figure 15: Transverse displacement of the free end [12]

When $V = 0\,m/s$, and not considering material damping, the system presents sharp resonances corresponding to the theoretical natural frequencies. When the fluid is flowing, the response is smoother because of the damping forces originated by the fluid flow. This response is close to the response obtain by [12] model, only differing on the response for low frequencies when $V = 50\,m/s$. This difference might be caused by the authors model since the static displacement ($f = 0Hz$) only involves the stiffness matrix and force vector for the displacement calculation, and, since with the increase in

flow velocity through the pipe, the overall stiffness decreases and the static deflection is increases. So the higher the flow velocity, the higher the first data point in figures 14 and 15 should be.

4.3. Acoustic Results

In order to verify the acoustic model, and with the lack of literature results, *OpenPulse* [2] software was used to, first validate the code developed and second to check the differences in implementation. Given the L pipe with a prescribed pressure at one end and a volume velocity at the other end the pressure response and structural response can be compared. For this the node containing the prescribed volume velocity is used. The pressure response is presented in figure 16 and the structural response is in figure 17.

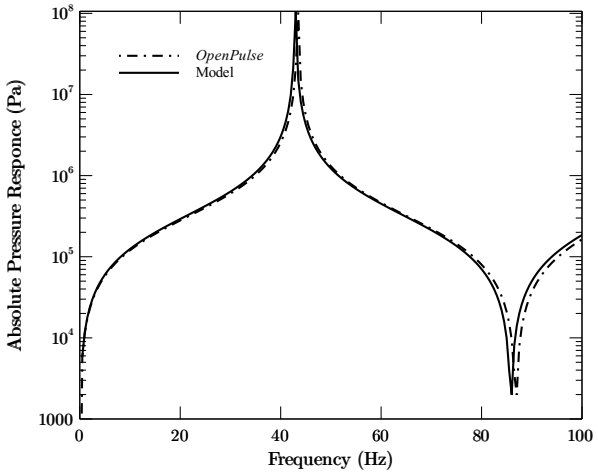

Figure 16: Acoustic pressure response in the free end with pressure boundary conditions and volume velocity at each end

there is no significant pressure field difference between models so one of the explanations possibles has to do with the formation of the force vector or the formulation of fluid mass matrix. Since the lines in figure 17 are shifted only in the vertical direction the most probable cause is the formulation of the force vector, because in the model developed, for each frequency, free node displacement is less than the *OpenPulse* model.

4.4. *OpenPulse* Industrial Example

Figure 18 shows a pipe system, a structural frame and a beam supporting the large chamber on the left side of the image. The ends of the frame and supporting beam are clamped to ground, and the pipe is connected to the frame beams through elastic links.

Figure 19 only shows the pipe system. A compressor excitation is placed in pipe at the node at the bottom of the figure (node with lowest z coordinate) and all the other pipe endings are connected to other pipe network sections.

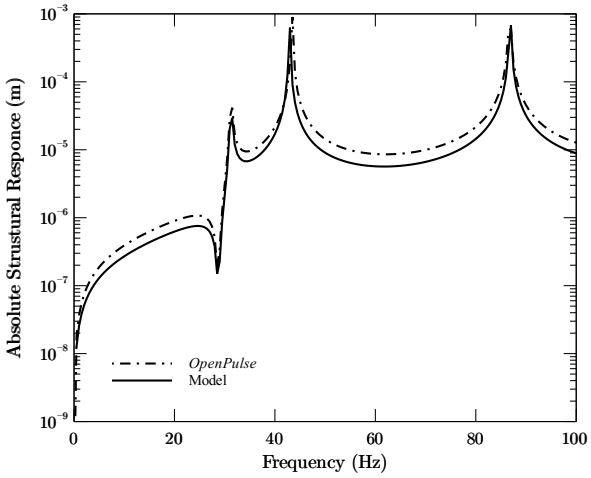

Figure 17: Structural response of the free end given the pressure field

Figure 18: Industrial example with pipe system and structural frame

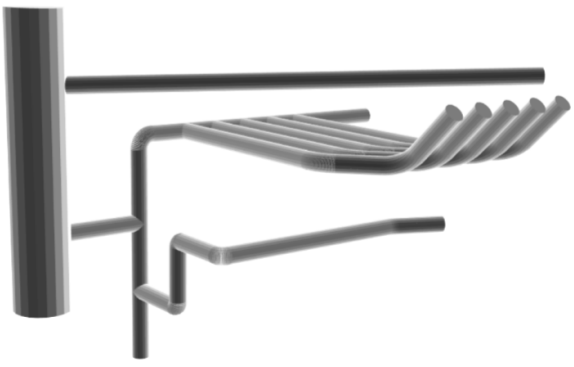

Figure 19: Industrial example with pipe system

With every element represented with 3 elements and each corner with 5 elements, the final mesh is displayed as figure 20. This mesh is imported by the user that gives the relevant node coordinates, connectivity and refinement parameters.

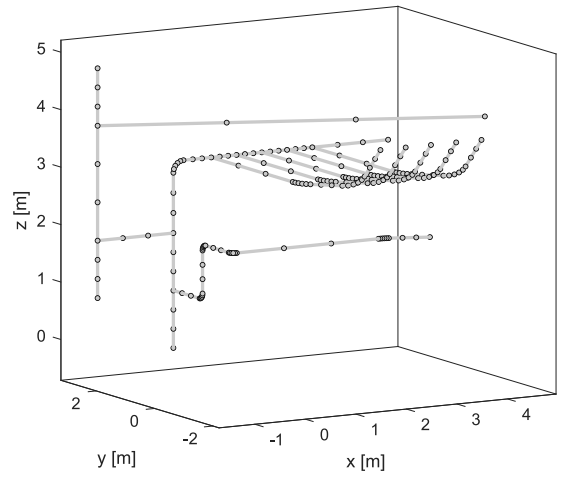

Figure 20: Pipe network in MATLAB with refinement

Performing an harmonic acoustic analysis the absolute pressure response at node 6 is given by figure 21. This result is very similar to the one computed with *OpenPulse* and with a mesh composed with 251 nodes compared with more than 6000 nodes used in *OpenPulse*.

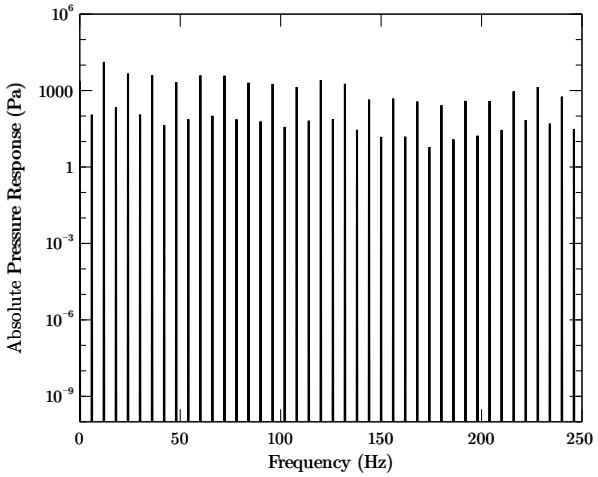

Figure 21: Compressor node absolute pressure response

5. Conclusions

Considering Euler-Bernoulli and Timoshenko developed models compared to the analytical solution for simple beams with common boundary conditions it can be seen that the number of element necessary of archive a precise result increases with the increase of frequency mode number, for both models. The distinction between models stiffness is very clear an it can be seen that with the increase of mode number the difference between models lets bigger. As the pipe thickness-to-length ratio reduces differences between models are not significant, however that ratio gets larger the differences in models and their application are evident. In more complex pipe designs, model validation was perform with the use of *OpenPulse* where it was concluded that the developed models results, both natural frequencies and modes of vibration, are very close to the ones in *OpenPulse*.

Different models to characterize a pipe system with steady internal flow exist. Many of those models approach to the same problem differ but all the models analysed in this thesis are very close to the one developed, for straight pipes and curved pipes. A comparison between the model and a laboratory experiment [11] proved that the model follows the experimental data with high precision.

For the acoustic results a comparison between the developed model and *OpenPulse* was performed. The pressure field was calculated for different pressure and volume velocity boundary conditions. The results show an high precision in pressure at different nodes. Given the calculated pressure field the coupled force vector has calculated and the structural response presents an error compared with *OpenPulse*. This error is only associated with the absolute response for a given frequency. This means a difference in the calculation of force vector between the models exist, but the model developed is capable of being used to calculate pressure fields and structural response of a pipeline excited by a compressor.

The pressure field calculated for an complex industrial example is a good evidence of the model precision given an compressor flow rate source. This example also provided a good opportunity to check that the mesh processing algorithm developed is capable of model very complex pipe network.

When performing an structural analysis with steady internal flow some problems arise from the model developed. Since the user can only enter one value for the fluid velocity, in more complex pipe networks, internal velocity will change based on the amount of branches or connections, also assuming no change in cross-section area along the network. One method to solve this issue is to define the velocity for a given length section. In a branched T element the user must be able to define three different velocities with mass conservation in mind. This is not recommended to do automatically because depending on the T angle between tubes and pres-

sures at each of the segments, the calculation of the exit velocity for two of the pipes is very complicated only with an input velocity.

Pressure effects can also be implemented and with this an transient analysis should be performed to, because since we are dealing in steady flow, the fluid-structure interaction forces are constant. Those interactive forces can now contain the change in fluid momentum, not implemented in the acoustic coupled analysis, because of the already known velocities across system. Given this information, friction coupling mechanism can also be modeled with ease, first because the direction of that force is coincident with velocity vector and because this force can be easily computed with fluid and pipe surface properties.

In acoustics developed code, some improvements can be performed. First different pipe elements can be implemented, such as side branches, a large volume pipe and a resistance that decreases pressure across it. This can be performed by changing the global mobility matrix based on the different elements local mobility matrices. The same improvement given for the fluid-structure interaction detailed above can be implemented for this analysis. The major problem is the need to solve the volume velocity field for the entire system to be able to modify the coupled force vector to account for change in fluid momentum.

Acknowledgements

I thank Professor Miguel Matos Neves from Instituto Supeior Técnico for having accepted me to carry out this project and for all assistance provided since the beginning. I would also like to thank to Dr. Olavo M. Silva for the help provided in crucial stages of this project with the knowledge and experience in the acoustic part of this thesis.

References

[1] Peixin Gao, Tao Yu, Yuanlin Zhang, Jiao Wang, and Jingyu Zhai. Vibration analysis and control technologies of hydraulic pipeline system in aircraft: A review. *Chinese Jornal of Aeronautics*, 34(4):83–114, 2021.

[2] O. M. Silva, D. M. Tuozzo, J. G. Vargas, L. V. Kulakauskas, A. F. Fernandes, J. L. Souza, A. P. Rocha, A. Lenzi, R. Timbo, C. O. Mendonca, and A. T. Brandao. Numerical modelling of low-frequency acoustically induced vibration in gas pipeline systems. Technical report, Federal University of Santa Catarina, Multidisciplinary Optimization Group, MOPT/LVA, Campus Trindade, Florianópolis, Brazil. Software Open Source GITHUB: https://github.com/openpulse/OpenPulse#readme.

[3] Eugenio Oñate. *Structural Analysis with the Finite Element Method. Linear Statics*, volume 2. CIMNE, 1^{st} edition, 2013. ISBN:978-1-4020-8742-4.

[4] Lars Andersen and S. R. K. Nielsen. Elastic beams in three dimensions. Aalborg University - DCE Lacture Notes No. 23, August 2008.

[5] Robert D. Blevins. *Flow-Induced Vibration*. Krieger Publishing Company, 2^{nd} edition, 2001. ISBN:1-57524-183-8.

[6] C. S. W. Lavooij and A. S. Tijsseling. Fluid-structure interaction in liquid-filled piping systems. *Jornal of Fluids and Structures*, 5:573–595, 1991.

[7] A. S. Tijsseling. Fluid-structure interaction in liquid-filled piping systems: A review. *Jornal of Fluids and Structures*, 10:109–146, 1996.

[8] A. J. M. Ferreira. *MATLAB Codes for Finite Element Analysis - Solids and Structures*, volume 157 of *Solid mechanics and its applications*. Springer, 2009. ISBN:978-1-4020-9199-5.

[9] Daryl L. Logan. *A First Course in the Finite Element Method*. Cencage Learning, 6^{th} edition, 2016. ISBN-13:978-1-305-63734-4.

[10] Mamoru Tanaka and Katsuhia Fujita. Vibration of piping system by pulsation of containing fluid. (in Japanese).

[11] Harold L. Dodds and Harry L. Runyan. Effect of high-velocity fluid flow on the bending vibrations and static divergence of a simply supported pipe. *NASA TN D-2870*, June 1965.

[12] N. Piet-Lahanier and R. Ohayon. Finite element analysis of a slender fluid-structure system. *Journal of Fluids and Structures*, 4:631–645, 1990. doi:0889-9746/90/060063.